

Monolithic Microchannels in Miniature Pneumatic Soft Robots for Sequential Motions

Dongliang Fan[†], *Member, IEEE*, Hao Liu[†], Ting Wang, Renjie Zhu, *Graduate Student Member, IEEE*,
and Hongqiang Wang*, *Senior Member, IEEE*

Abstract—Miniature soft robots present great potential in delicate manipulations due to their gentle force, compliant structures, and flexible motions. Easy control and fast response make pneumatic actuation a prevalent method for driving soft robotics. In addition, sequential motions are also crucial for enhancing the grasping and moving abilities of soft robots. However, existing miniature pneumatic soft robots are limited to one-dimensional geometries and simple motions due to the difficulties in designing and fabricating intricate small airways in miniature pneumatic soft robots, which restricts them from more versatile deformations. Here, we employ intricate monolithic microchannels embedded into miniature soft robots' monolithic bodies for sequential motions. After verifying the effects of the channel diameter, strain-limiting layer, and elastic modulus of the robot's body on the bending behaviors of the 1D soft robots, we fabricated a soft flower robot capable of sequential and simultaneous 3D-to-3D shape morphing through five individual microchannels and a soft carnivorous plant robot containing 2D interconnected microchannels capable of sequential enclosed grasping through a single inlet.

I. INTRODUCTION

Soft robots can readily achieve versatile operations, including interacting with fragile objects [1], exploring unknown environments [2], and mimicking the motions of animals or plants [3, 4] due to their excellent compliance for safe interaction [5]. Miniature soft robots become promising solutions to realizing safe navigation, delicate manipulation, and precise operation [6], which are essential to specific scenarios, including minimally invasive surgeries [7], fragile creature capturing [8], and cargo release tasks [9]. In recent decades, different approaches have been proposed for actuating small-scale soft robots. Electrostatic actuation has exhibited excellent performance in rapid response, strong output force, and precise displacement, still, the high voltage remains a potential danger when interacting with humans [10, 11]. Magnetic actuation endows the miniature soft robots with untethered operations and fast response. However, magnetic soft robots require complex control systems for actuating and are only applicable in confined environments [12]. In addition,

[†] Equally contributing authors. Corresponding author: Hongqiang Wang.

Dongliang Fan, Hao Liu, Ting Wang, Renjie Zhu, and Hongqiang Wang are with the Shenzhen Key Laboratory of Intelligent Robotics and Flexible Manufacturing Systems, Southern University of Science and Technology, Shenzhen, 518055, China.

This work was supported by the National Natural Science Foundation of China under Grant 52275021, the National Key R&D Program of China under Grant 2022YFB4701200, the Science, Technology, and Innovation Commission of Shenzhen Municipality under Grant ZDSYS20200811143601004 and ZDSYS20220527171403009, the Southern Marine Science and Engineering Guangdong Laboratory (Guangzhou), under Grant K19313901.

thermal actuation still lacks the ability for fast actuation due to the slow heat dissipation process [13].

Pneumatic actuation is prevalently employed for achieving various tasks due to the simple setup, easy control, and fast response [14]. Moreover, pneumatic soft robots require simple structures, soft matrices with internal voids, and easy fabrication, bonding the cast elastic structures (soft lithography) [15]. One-dimensional (1D) pneumatic soft robots have already achieved bending and twisting deformations on a small scale [16-18]. However, the rupture always occurs at the joint region, and defects, such as small cylindrical pillars, are seldom avoided when adhering two parts together, especially at several hundred microns, where surface tension plays a dominant role [8]. Monolithic microchannels have been employed in 1D pneumatic soft robots, which can bear pressure up to 70 kPa [17]. But their fabrication methods are applicable to simple geometries, which limits the design flexibility for performing more complex deformations of soft robots. Additive manufacturing is able to fabricate soft millimeter-scale grippers with intricate geometries due to its high design flexibility [19, 20]. But its long fabrication duration and post-processing for UV-cured resin are not applicable for the scalability and mass production for miniature soft robot generation.

Moreover, sequential motions are essential for biological systems, such as the running of animals requiring the synergic movement of their limbs and carnivorous plants controlling the sequential bending of their leaves during the capturing process. In addition, sequential motions are also crucial for the grasping and moving performances of soft robots. The complex moving gaits for a soft quadrupedal robot [21] and delicate in-hand manipulation for robotic hands [22] were realized by controlling the individual pneumatic channels. Therefore, sequential motions can benefit and enhance the deforming ability for more complex operations of soft robots. Besides connecting multiple inputs, to reduce the control complexity and avoid redundancy pipelines, which may hinder the motions of soft robots, different approaches, such as harnessing the viscous flow by optimizing the diameter and length of the connecting tubing [23], and employing additional devices, i.e., a fluidic relaxation oscillator [24], multiple capillary orifices [25], and a soft pneumatic valve [26], have been taken to achieve a single output source for sequential movements. In addition, thickness difference was employed for sequential actuation of the soft digits with one monolithic channel by a single pressure input [18]. However, these existing strategies are not applicable for achieving sequential motions in monolithic small-scale pneumatic soft robots since these robots always require flexible tubing to

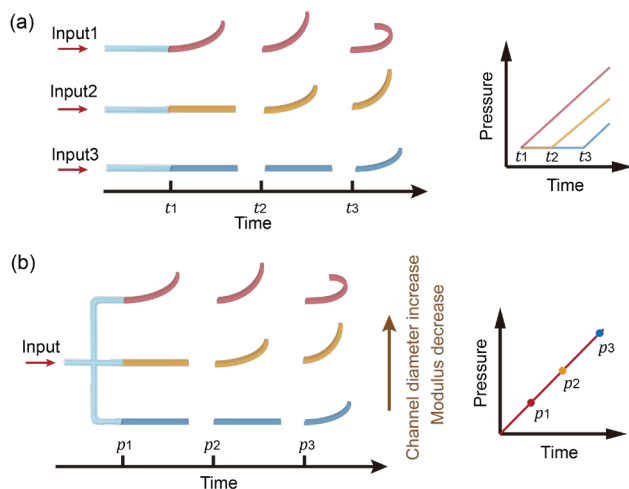


Fig. 1 Sequential motions strategies for soft robots. (a) Multiple pressured air inputs for sequential motions with initiating time difference. (b) Single input for sequential motions with initiating pressure difference.

connect individual parts of robots, and the external components, such as valves, are difficult for miniaturization and integration into soft bodies of the soft robots.

Herein, we propose a strategy by designing and employing intricate monolithic microchannels into miniature soft robots for sequential motions. Compared to bonding two soft parts for airways generation, we selected the soft demoulding method proposed in our previous work for fabricating monolithic microchannels in elastic matrices due to the simple fabrication process [27]. The monolithic microchannels can not only work as the actuating channels but serve as the air transporting pipeline, improving the integration of the soft robots. The channel diameter and elastic modulus of the matrix are tunable for realizing different actuating pressures. Two approaches are presented for the sequential motions of soft robots (Fig. 1). The first approach employs multiple pressured air inputs, and sequential motions can be realized by controlling the time delay among the inputs (Fig. 1(a)). The other introduces interlaced channels with a single inlet. The

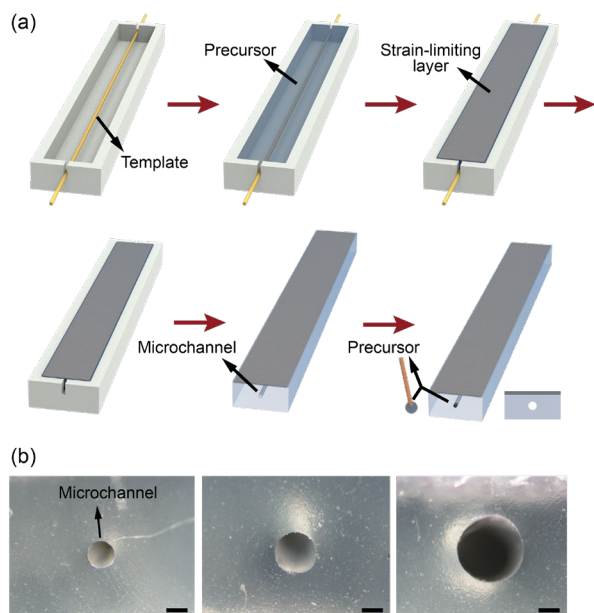


Fig. 2. 1D soft miniature robot. (a) Fabrication process of the 1D soft robot. (b) Cross sections of the soft robots. Scale bar, 200 μm .

different initiating pressures of these channels for deformation are achieved by the differences in channel diameter and elastic modulus (Fig. 1(b)). We first performed a series of experiments to test the 1D soft robots' bending performance and verify the effects of the microchannel diameter, without a strain-limiting layer, and elastic modulus of the soft matrix on the actuating pressure for miniature soft robots (dimension: 2 mm \times 4 mm \times 40 mm). Finally, we prepared two demonstrations through the distribution of the monolithic microchannels in the soft robots: a soft flower robot capable of sequential and simultaneous closing its petals through inflating five separated 3D microchannels and a soft carnivorous plant robot capable of sequential grasping through one inlet due to the difference in actuating pressure for the 2D interconnected microchannels with different diameters and elastic modulus.

II. METHOD

A. Design and fabrication of 1D miniature soft robots

Soft lithography, the most common fabrication method for miniature soft robot generation, has been employed for versatile, delicate grasping applications. However, this technology requires adhering a flat layer onto a layer with a void to produce the channel structure. The weak bonding force makes the interface susceptible to bursting when inflated. Defects (i.e., pillars in channels) generated during the bonding process limit the bending performance of soft robots. Herein, we chose soft demoulding technology for fabricating miniature pneumatic soft robots due to the straightforward, fast, robust fabrication process for monolithic microchannel generation.

For pneumatic soft robots, the bending motion requires a bending stiffness difference in the top and bottom sides of the actuating channel. Most of the differences are achieved by asymmetric thicknesses and strain-limiting layers. In our experiments, the asymmetric thickness and strain-limiting layer are employed in the soft robots. Here, we showed the fabrication process of the 1D soft robot with a strain-limiting layer as an example. A thermoplastic polyurethane (TPU) filament generated by thermal extrusion from a 3D printer nozzle (RAISE3D E2) was first fixed in a 3D-printed mold (printed by RAISE3D E2, nozzle diameter: 0.4 mm, printing layer accuracy: 0.1 mm). Then, the elastomer precursor, prepared by mixing equal mass of part A and part B (Ecoflex 50, Smooth-On) and degassing for 5 minutes, was poured into the mold. After that, a cotton fabric strip (thickness: 200 μm) soaked with the elastomer precursor working as the strain-limiting layer was attached to the top of the mold, and the

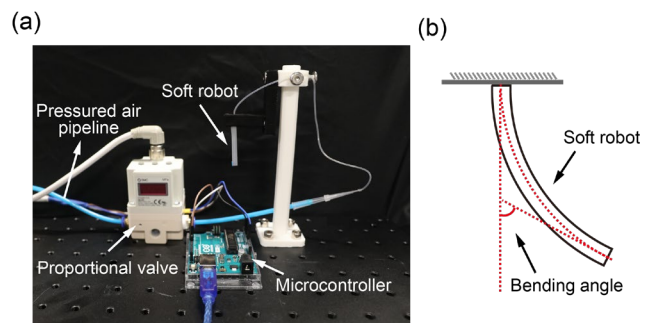


Fig. 3. Bending angle test of the soft robot. (a) Actuation setup for the soft robot. (b) Bending angle definition.

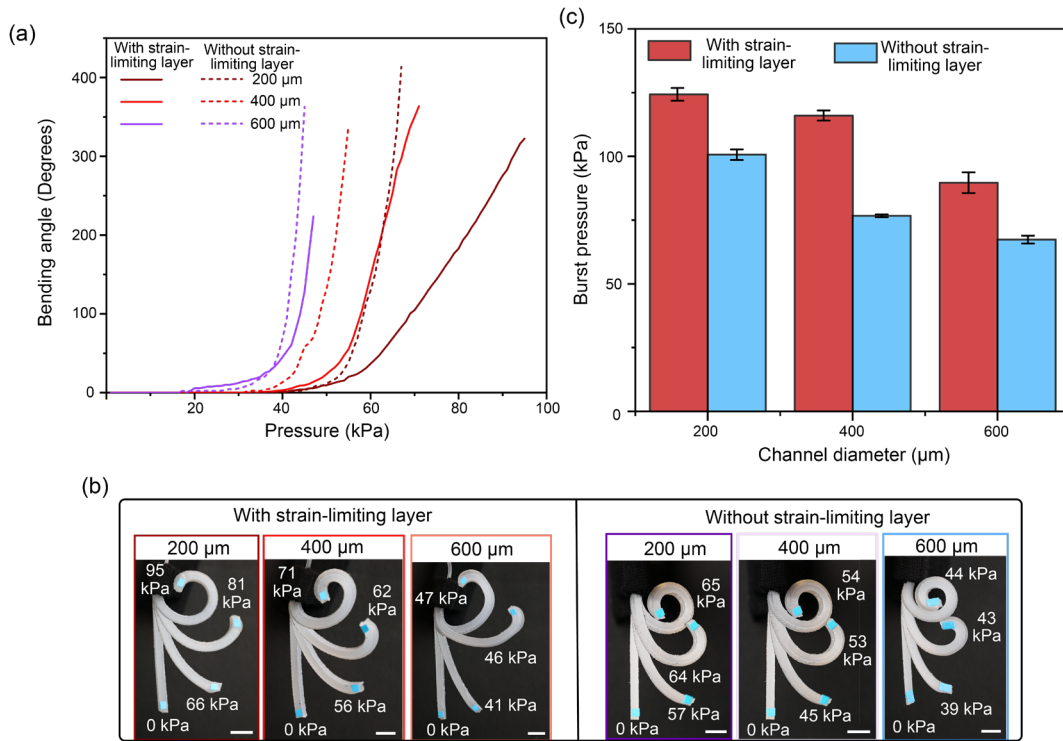


Fig. 4. Effect of microchannel diameter on the bending behavior of soft robots with and without strain-limiting layer. (a) The relationship between applied pressure and bending angle with different microchannel diameters for soft robots with and without strain-limiting layer. (b) The bending process of soft robots with and without strain-limiting layer. Scale bars, 5 mm. (c) Burst pressure as the function of microchannel diameter.

precursor was thermally cured. Next, the filament was demolded from the elastic matrix, and the elastic matrix was detached from the mold. Finally, a small amount of precursor was used to block the front end of the microchannel to form a 1D miniature pneumatic soft robot, as shown in Fig. 2(a). Following a similar protocol, a series of soft robots containing microchannels with different diameters, 200, 400, and 600 μm, were demonstrated in Fig. 2(b).

III. EXPERIMENTAL RESULTS

A. Parameters for bending behavior control of 1D soft robots

Exploring the effect of microchannel diameters, strain-limiting layers, and elastic modulus of the elastic materials is crucial to controlling the bending behaviors of pneumatic soft robots. The 1D soft robot with the dimensions 40 mm in length, 4 mm in width, and 2 mm in thickness was designed for the following bending behavior tests. The actuating and

measuring setup was designed as shown in Fig. 3(a). The compressed air was inflated into the microchannel of the soft robot through a proportional valve, and the real-time pressure was tuned by the microcontroller. The definition of the bending angle of 1D soft robots is shown in Fig. 3(b). The bending process of the soft robots was recorded by the camera (5D4, Canon), and the bending angle was acquired through our image processing algorithm [28]. To verify the effect of microchannel diameter on the bending behavior of soft robots, we employed three different microchannels, 200, 400, and 600 μm, in the soft robots. The microchannel diameter can be tuned by varying the filament template. We observed an increasing actuating pressure required for achieving the same bending angle as the microchannels of the soft robots decreased (see Fig. 4(a)) for both soft robots with and without the strain-limiting layer, and the bending sequences were shown in Fig. 4(b). In this test, the soft robot with a larger diameter requires a smaller actuating pressure to realize a

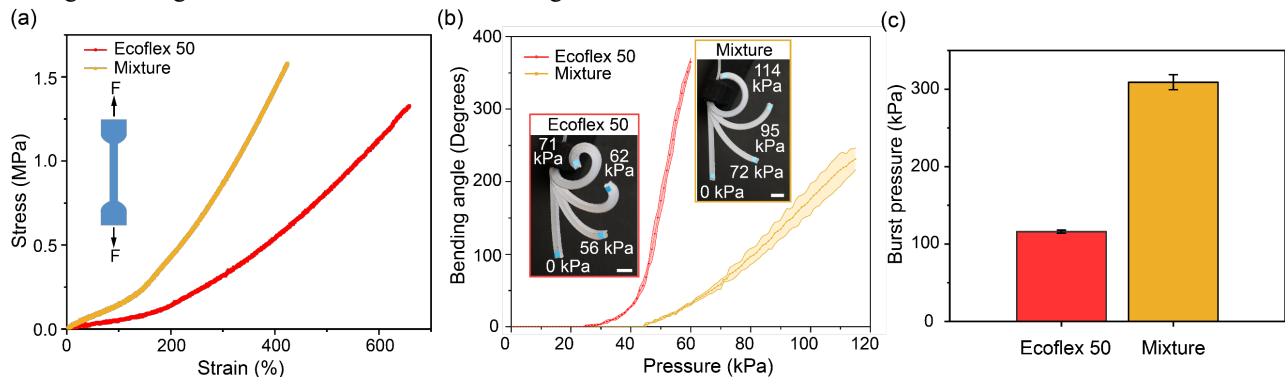


Fig. 5. Effect of elastic modulus of the soft matrix on the bending behavior of soft robots. (a) The stress-strain curves of the elastic matrix. (b) The relationship between applied pressure and bending angle with different materials. The insets show the bending process of soft robots. Scale bars, 5 mm. (c) Burst pressure as the function of soft matrix's elastic modulus.

similar bending angle due to its smaller area moment of inertia and larger bending torque. The burst pressure of the soft robots was measured by increasing the inflating pressure till the robot ruptured, and the burst pressure was recorded. Similarly, the burst pressure decreases as the channel diameter increases (Fig. 4(c)).

In addition, the soft robots with and without a strain-limiting layer (cotton fabric with 200 μm in thickness) were also analyzed for the bending behavior of the soft robots. The matrix material (Ecoflex 50) was kept constant for the soft robot without a strain-limiting layer. The stiffness difference of the soft robot without a limiting layer is realized by the asymmetric thickness on both sides of the microchannel (600 μm thickness difference). The pure soft robot requires smaller actuating pressure to achieve the same bending angle and smaller burst pressure due to the smaller bending stiffness compared to the robot containing a strain-limiting layer, as shown in Fig. 4(a). The bending performance deviation of the soft robots may cause by the assembly error of templates, which determines the location of the microchannels.

B. Elastic modulus of the soft matrix

The effect of the elastic modulus of the soft matrix was validated by using two different materials (Ecoflex 50 and Mixture), and the microchannels (diameter: 400 μm) of the soft robots were kept constant. The Mixture was prepared by adding part A, part B of Dragon skin 30 precursors, and part A, part B of Ecoflex 30 precursor into a beaker in sequence (the volume ratio of Dragon skin 30 and Ecoflex 30 precursor: 1:1). The stress-strain tests were performed to measure the elastic modulus of the materials, and the Mixture exhibited a higher modulus (Fig. 5(a)). The more rigid Mixture requires a larger bending torque for the 1D soft robots; therefore, a higher pressure was required to actuate and burst the soft robots, which coincides with our experimental results (Fig. 5). These validated parameters for tuning the actuating pressure for soft roots are critical to our strategy for sequential motions in the following demonstrations.

C. Sequential motions of the soft flower robot via 3D independent microchannels

3D reversible morphing capabilities are widely existing in plants and animals for moving, capturing, and camouflaging, such as swimming of a jellyfish and closing its petals of a soft flower. These sophisticated motions are realized through the 3D-distributed soft tissues in these living creatures [29-30]. Inspired by the morphing abilities of these creatures, researchers have proposed employing complex strain-limiting

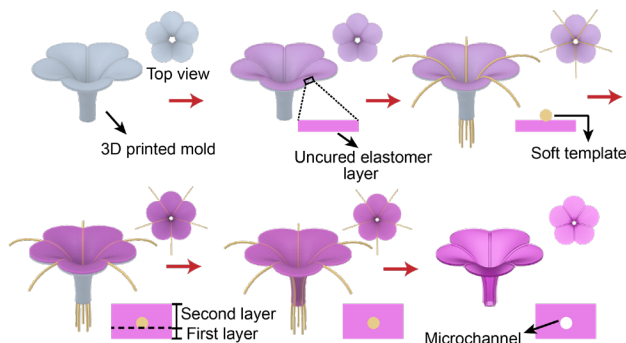


Fig. 6. Fabrication process of the soft flower robot.

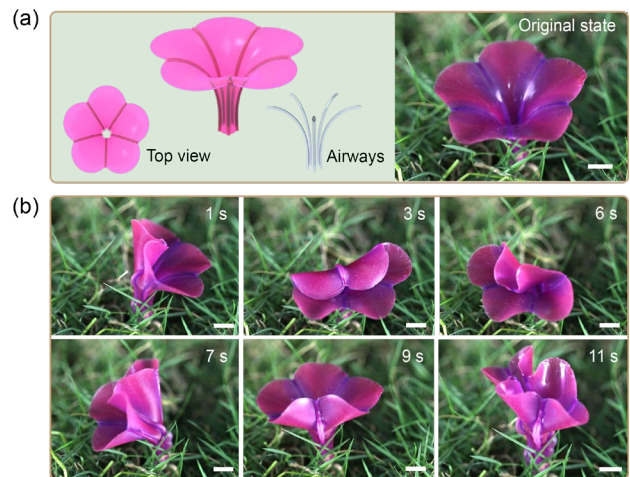


Fig. 7. Sequential bending of the soft flower robot. (a) Schematic and original state of the soft robot. (b) The sequential bending and simultaneous bending of the soft flower robot. scale bars, 5 mm.

layers, i.e., synthetic tissue patterns [22] and kirigami plastic shells [31], and intricate 2D airway networks [32] in the elastic layers for achieving the programable deformations from planar geometries into the 3D configurations. Here, to better imitate the morphology and 3D deforming capability of flowers, we embedded 3D monolithic microchannels into the soft flower robot to achieve 3D-to-3D shape morphing. The 3D distributed microchannels resemble the soft tissues in the soft flowers for controlling their motions. In addition, the microchannels are designed into individual parts, which are applicable for independent control of each petal of the soft flower robot.

The fabrication of the pneumatic soft flower robot containing 3D microchannels is still challenging. Soft lithography is not capable of fabricating 3D microchannels for 3D geometrical soft robots due to its fabrication limitations. Inspired by the coating of the slender elastic shells on curved surfaces [33], we fabricated the soft flower robot by employing the inner coating of a flower-shaped mold, and the thickness difference was taken for achieving the bending performance due to the gentle actuating pressure. The fabrication process was discussed in detail as follows: a dyed silicone precursor (Ecoflex 0050, Smooth-on) was first poured into a 3D printed flower-shaped hollow mold with five grooves inside, and a thin precursor remained on the mold surface. Before the silicone precursor was completely cured at room temperature (waiting duration: 1 hour), five TPU

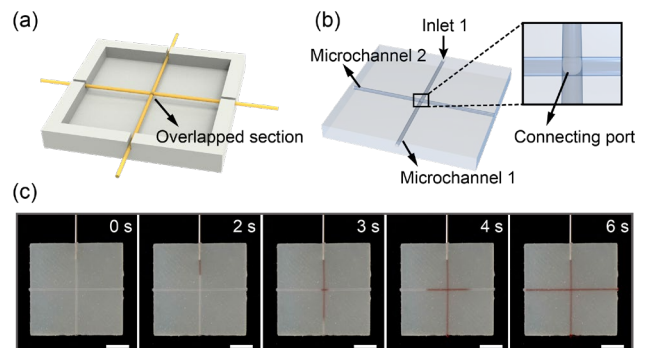


Fig. 8. Interconnected microchannels. (a) The template filament distribution during the fabrication process. (b) Schematic of the interconnected microchannel. (c) The flow process of the red ink from Microchannel 1 to Microchannel 2. Scale bars, 5 mm.

filaments (diameter: 400 μm) were attached to the silicone precursor. The waiting duration before attaching the filaments is crucial to the monolithic microchannel fabrication since the viscosity of the precursor should be large enough to support the filament and able to build a strong interface when another precursor layer is cast. Then, the precursor was poured into immersing the template, and then a second layer was cast on the parts containing filaments to generate a thicker elastic layer after curing at room temperature. After the elastic matrix was detached from the mold, five independent 3D microchannels were created inside of the elastomer after the templates were removed from the matrix. Finally, the top ends of the microchannels were sealed by a small volume of precursors, and the soft flower robot was generated, as shown in Fig. 6.

To exhibit the sequential motion ability of our soft flower robot, each of the five microchannels was connected to an air source for providing pressured air via independent silicone tubing. In our demonstration, each of the five petals of the soft robot bent in sequence when inflating the corresponding microchannels. Moreover, the simultaneous bending of the five petals was also realized when the five microchannels were actuated simultaneously, as shown in Fig. 7.

D. Sequential motions of the soft robot via interconnected microchannels

Sequential motions are important for soft robots to perform certain tasks, including running, swimming, and camouflaging. In general, these soft robots consist of individual actuating chambers. To generate complex and sequential motions, each chamber in the soft robots requires individual actuating (pressurized air sources) and control systems (valves), just like the actuating process of our soft flower robot mentioned above. The multiple input lines connecting to the bodies of soft robots may limit the robots' moving ability and require complex control systems for

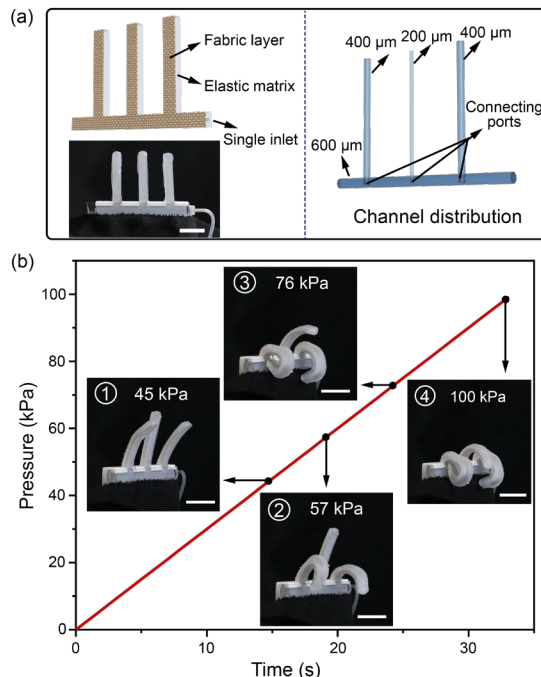


Fig. 9. Sequential bending of the soft robot with three digits. (a) Schematic and microchannel distribution of the soft robot. (b) The sequential bending of the three soft digits. scale bars, 10 mm.

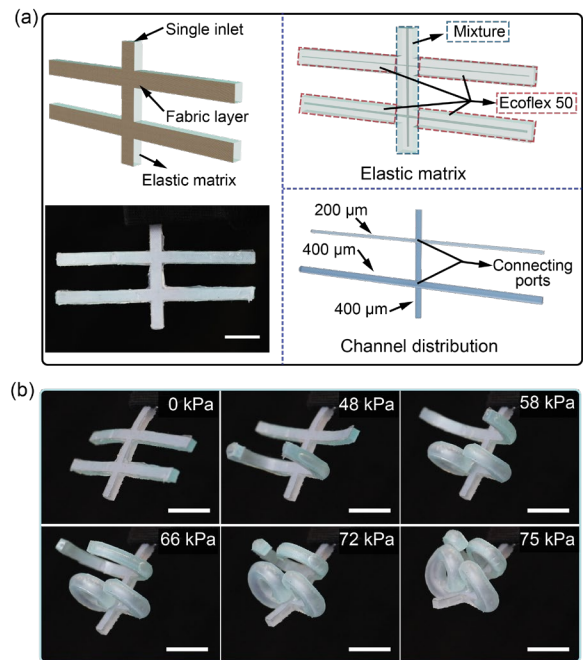


Fig. 10. Sequential bending of the soft camivorous plant robot. (a) Schematic, elastic matrix, and microchannel distribution of the soft robot. (b) The sequential motion of the soft robot. scale bars, 10 mm.

achieving sequential motions [21]. Here, we avoid adding external components, such as fluidic oscillators and extra connecting tubing, and harness the interconnected microchannels with a single inlet in the soft robots. The sequence motions are achieved by the difference in the actuating pressure of individual microchannels due to the variation in microchannel diameter and the strain-limiting layer of each microchannel.

The design and fabrication of interconnected microchannels are crucial to soft robots. Additionally, based on our fabrication method, the 1D filament is hard to generate planar interconnected microchannels. Herein, we employed interlaced 1D filaments with overlapped sections during the fabrication process. After removing the filaments from the elastic matrix, the overlapped sections generate a connecting port between microchannels, which is an applicable approach to fabricating interconnected microchannels for soft robots. We validated this approach by injecting the red ink through Inlet 1 of Microchannel 1, and the inks flowed into Microchannel 2 through their connecting port with a small lag after the matrix was treated by air plasma due to the capillary interaction, as shown in Fig. 8.

To verify the sequential bending ability of soft robots containing multiple connected microchannels with a single inlet, we fabricated a soft robot with three digits. This soft robot contains four microchannels: the horizontal microchannel (diameter: 600 μm) works as the air transporting channel, one end of which was connected to a pressure source, and this microchannel contains individual connecting ports with other three microchannels; three actuating microchannels (diameters: 400 μm , 200 μm , and 400 μm respectively) in the three soft digits, as shown in Fig. 9(a). We applied a rigid frame to the horizontal microchannel to confine its deformation due to the largest diameter being first vulnerable to bending when inflating. As the pressure increased, the left and right soft digits were bending

simultaneously with a similar bending angle due to the same microchannel diameter. In addition, the middle soft digit presented a delayed bending process since its microchannel diameter was smaller, as shown in Fig. 9(b).

Finally, inspired by the trapping motion of the carnivorous plant (*Drosera capensis*) [29], we designed and fabricated a soft carnivorous plant robot to achieve the sequential motion of their individual leaf for preying through a single inlet, as shown in Fig. 10. In this demonstration, we employed different diameters of the microchannel (200 and 400 μm) and elastic materials (Ecoflex 50 and Mixture) for realizing the sequential bending process. The horizontally distributed microchannels were embedded in the same matrix (Ecoflex 50), and the larger diameter (400 μm) presented an earlier bending process. In addition, the vertical microchannel was embedded into a more rigid elastic matrix (Mixture) and exhibited the latest bending after the pressure is excess of 58 kPa. As the pressure increased, the two side leaves bent sequentially, and then the middle leaf also bent to realize the enclosed grasping (Fig. (10b)).

IV. CONCLUSIONS

This paper presents a new approach to the sequential motions of miniature soft robots by introducing intricate monolithic microchannels in the robots' bodies. We validated our strategy by a soft flower robot with five individual microchannels actuating by five pressure sources. A soft carnivorous plant robot containing interlaced microchannels for sequential bending resembling the capturing process of the natural carnivorous plant, was also generated.

Future works include modeling and quantitative analysis of the bending behaviors, programmable design of the intricate microchannels, and involving more versatile motions, including elongation and rotation, into soft robots.

REFERENCES

- [1] D. Li et al., "Origami-inspired soft twisting actuator," *Soft Robotics*, vol. 10, no. 2, p. 395-409, 2023.
- [2] E. W. Hawkes, L. H. Blumenschein, J. D. Greer, and A. M. Okamura, "A soft robot that navigates its environment through growth," *Science Robotics*, vol. 2, no. 8, p. eaan3028, 2017.
- [3] R. Zhu et al., "Soft Robots for Cluttered Environments Based on Origami Anisotropic Stiffness Structure (OASS) Inspired by Desert Iguana," *Advanced Intelligent Systems*, p. 2200301, 2023.
- [4] Q. Shao et al., "Untethered Robotic Millipede Driven by Low-Pressure Microfluidic Actuators for Multi-Terrain Exploration," *IEEE Robotics and Automation Letters*, vol. 7, no. 4, pp. 12142-12149, 2022.
- [5] O. Yasa et al., "An Overview of Soft Robotics," *Annual Review of Control, Robotics, and Autonomous Systems*, vol. 6, 2022.
- [6] D. Fan et al., "Innervation of Sensing Microchannels for Three - Dimensional Stimuli Perception," *Advanced Materials Technologies*, p. 2300185, 2023.
- [7] T. Gopesh et al., "Soft robotic steerable microcatheter for the endovascular treatment of cerebral disorders," *Science Robotics*, vol. 6, no. 57, p. eabf0601, 2021.
- [8] N. R. Sinatra, C. B. Teeple, D. M. Vogt, K. K. Parker, D. F. Gruber, and R. J. Wood, "Ultragentle manipulation of delicate structures using a soft robotic gripper," *Science Robotics*, vol. 4, no. 33, p. eaax5425, 2019.
- [9] Q. Ze et al., "Soft robotic origami crawler," *Science Advances*, vol. 8, no. 13, p. eabm7834, 2022.
- [10] H. Wang et al., "Biologically inspired electrostatic artificial muscles for insect-sized robots," *The International Journal of Robotics Research*, vol. 40, no. 6-7, pp. 895-922, 2021.
- [11] C. Tang et al., "A pipeline inspection robot for navigating tubular environments in the sub-centimeter scale," *Science Robotics*, vol. 7, no. 66, p. eabm8597, 2022.
- [12] Y. Xing, D. Hussain, and C. Hu, "Optimized dynamic motion performance for a 5-dof electromagnetic manipulation," *IEEE Robotics and Automation Letters*, vol. 7, no. 4, pp. 8604-8610, 2022.
- [13] A. Miriyev, K. Stack, and H. Lipson, "Soft material for soft actuators," *Nature Communications*, vol. 8, no. 1, pp. 1-8, 2017.
- [14] R. V. Martinez et al., "Robotic tentacles with three - dimensional mobility based on flexible elastomers," *Advanced Materials*, vol. 25, no. 2, pp. 205-212, 2013.
- [15] S. Russo, T. Ranzani, C. J. Walsh, and R. J. Wood, "An additive millimeter - scale fabrication method for soft biocompatible actuators and sensors," *Advanced Materials Technologies*, vol. 2, no. 10, p. 1700135, 2017.
- [16] N. Sinatra, T. Ranzani, J. Vlassak, K. Parker, and R. Wood, "Nanofiber-reinforced soft fluidic micro-actuators," *Journal of Micromechanics and Microengineering*, vol. 28, no. 8, p. 084002, 2018.
- [17] Y. Sun, S. Song, X. Liang, and H. Ren, "A miniature soft robotic manipulator based on novel fabrication methods," *IEEE Robotics and Automation Letters*, vol. 1, no. 2, pp. 617-623, 2016.
- [18] T. J. Jones, E. Jambon-Puillet, J. Marthelot, and P.-T. Brun, "Bubble casting soft robotics," *Nature*, vol. 599, no. 7884, pp. 229-233, 2021.
- [19] Y. F. Zhang et al., "Miniature Pneumatic Actuators for Soft Robots by High - Resolution Multimaterial 3D Printing," *Advanced Materials Technologies*, vol. 4, no. 10, p. 1900427, 2019.
- [20] C. Tawk, G. M. Spinks, M. in het Panhuis, and G. Alici, "3D printable linear soft vacuum actuators: their modeling, performance quantification and application in soft robotic systems," *IEEE/ASME Transactions on Mechatronics*, vol. 24, no. 5, pp. 2118-2129, 2019.
- [21] R. F. Shepherd et al., "Multigait soft robot," *Proceedings of the National Academy of Sciences*, vol. 108, no. 51, pp. 20400-20403, 2011.
- [22] C. B. Teeple, R. C. S. Louis, M. A. Graule, and R. J. Wood, "The role of digit arrangement in soft robotic in-hand manipulation," in *2021 IEEE/RSJ International Conference on Intelligent Robots and Systems (IROS)*, 2021, pp. 7201-7208: IEEE.
- [23] N. Vasios, A. J. Gross, S. Soifer, J. T. Overvelde, and K. Bertoldi, "Harnessing viscous flow to simplify the actuation of fluidic soft robots," *Soft Robotics*, vol. 7, no. 1, pp. 1-9, 2020.
- [24] L. C. van Laake, J. de Vries, S. M. Kani, and J. T. Overvelde, "A fluidic relaxation oscillator for reprogrammable sequential actuation in soft robots," *Matter*, vol. 5, no. 9, pp. 2898-2917, 2022.
- [25] D. Paez-Granados, T. Yamamoto, H. Kadone, and K. Suzuki, "Passive flow control for series inflatable actuators: Application on a wearable soft-robot for posture assistance," *IEEE Robotics and Automation Letters*, vol. 6, no. 3, pp. 4891-4898, 2021.
- [26] C. J. Decker et al., "Programmable soft valves for digital and analog control," *Proceedings of the National Academy of Sciences*, vol. 119, no. 40, p. e2205922119, 2022.
- [27] D. Fan et al., "Self-shrinking soft demoulding for complex high-aspect-ratio microchannels," *Nature Communications*, vol. 13, no. 1, pp. 1-11, 2022.
- [28] https://github.com/lueluel23/Angle_detection_Visual-recognition
- [29] D. Panetta, K. Buresch, and R. T. Hanlon, "Dynamic masquerade with morphing three-dimensional skin in cuttlefish," *Biology Letters*, vol. 13, no. 3, p. 20170070, 2017.
- [30] C. A. La Porta et al., "Metamaterial architecture from a self-shaping carnivorous plant," *Proceedings of the National Academy of Sciences*, vol. 116, no. 38, pp. 18777-18782, 2019.
- [31] L. Jin, A. E. Forte, B. Deng, A. Rafsanjani, and K. Bertoldi, "Kirigami - inspired inflatables with programmable shapes," *Advanced Materials*, vol. 32, no. 33, p. 2001863, 2020.
- [32] E. Siéfert, E. Reysat, J. Bico, and B. Roman, "Bio-inspired pneumatic shape-morphing elastomers," *Nature Materials*, vol. 18, no. 1, pp. 24-28, 2019.
- [33] D. Fan et al., "Flow Casting Soft Shells with Geometrical Complexity and Multifunctionality," *Advanced Materials Technologies*, p. 2201640, 2023.